Mem. S.A.It. Vol. 82, 897

Memorie della

Cosmological cosmic ray production of LiBeB and PopIII stars

E. Rollinde and E. Vangioni

Institut d'Astrophysique de Paris, CNRS, UMR7095, UPMC Univ Paris 6, 98bis bd Arago, F-75014, Paris, France, e-mail: rollinde@iap.fr

Abstract. A new cosmological model of LiBeB production in the first structures has been performed. This was motivated by observations of ^{6}Li in halo Pop II stars that indicated a potentially high abundance of this isotope, about a thousand times higher than its predicted primordial value. Using a cosmological model for the cosmic ray-induced production of this isotope in the IGM allows us to explain the observed abundance at very low metallicity. Given this constraint on the ^{6}Li, we also calculate the non-thermal evolution with redshift of D, Be, and B in the IGM, and the resulting extragalactic gamma-ray background. The computation is performed in the framework of hierarchical structure formation considering several star formation histories including specifically Pop III stars. We find that spallative D production is negligible and that a potentially detectable Be and B plateau is produced by these processes at the time of the formation of the Galaxy (z∼3).

Key words. Nucleosynthesis: abundances – Stars: abundances – Stars: Population III – Stars: chemically peculiar – Cosmic Rays – Galaxy: abundances

1. Introduction

Big Bang Nucleosynthesis (BBN) together with Galactic Cosmic-Ray Nucleosynthesis (GCRN) have revealed a consistent picture for the origin and evolution of deuterium, helium, lithium, beryllium and boron. This combination involves very different aspects of nucleosynthesis including primordial, non-thermal and stellar nucleosynthesis, all of which are correlated through cosmic and chemical evolution. Until recently, there was one single free parameter in the standard model of BBN, the baryon density. Now this density has been determined with high precision by the observation of the cosmic microwave background (CMB) by the satellite WMAP (Komatsu et al., 2011) rendering BBN a parameter-free theory (Cyburt et al., 2008; Coc & Vangioni, 2010; Coc et al., 2011). The concordance between BBN theory at the WMAP value of the baryon-photon ratio, η, and the observation of D/H is a success of the Big Band standard model. Unlike deuterium, which is observed in high redshift quasar absorption systems, the LiBeB isotopes are observed in the atmospheres of stars in the halo of our Galaxy. D (and a part of ^{7}Li) is formed during BBN whereas ^{6}Li, ^{9}Be, and ^{10,11}B abundances are well explained in the context of GCRN (for a review see Vangioni-Flam et al., 2000). ^{7}Li is a complex isotope since it is synthesized in three astrophysical sites: BBN, GCR and stars.

Send offprint requests to: E. Rollinde

So, the most recent observations have led to two distinct Li problems. Firstly, given the baryon density inferred from WMAP, the BBN predicted value is ^{7}Li/H = 5.24±0.50 × 10^{-10} (Coc & Vangioni, 2010). It is significantly larger than determinations of the lithium abundance in Pop II stars which are in the range $1 - 2 \times 10^{-10}$ (Sbordone et al., 2010; Spite & Spite, 2010, and citations therein). This discrepancy is an open question which will not be addressed in this paper. Secondly, some observations of ^{6}Li at low metallicity (Asplund et al., 2006; Inoue et al., 2005) indicate a value of ^{6}Li/H = $10^{-11.2}$ which appears to be *independent* of metallicity in sharp contrast to what is expected from GCRN models, and is more consistent with a pre-galactic origin. While BBN does produce a primordial abundance of ^{6}Li (^{6}Li/H~10^{-14} Hammache et al., 2010) it is at the level of about 1000 times below these recent observations. However, Cayrel et al. (2007) and Steffen et al. (2010) have pointed out that line asymetries similar to those created by a ^{6}Li blend could also be produced by convective Doppler shifts in stellar atmospheres. Presently, a more detailed analysis is thus necessary to firmly conclude about the detection of the ^{6}Li abundance at this level in these metal poor stars.

Real or spurious, a pre-galactic formation of ^{6}Li is linked to other cosmological questions of interest. Such a non-thermal production of ^{6}Li must be related to an early population of massive stars and to the production of high-redshift *Cosmological Cosmic-Rays* (CCRs), accelerated by the winds of Pop III Super Novae (SN). Rollinde et al. (2006, hereafter RVOI) have investigated how a star formation history model in a cosmological context is able to explain this high level of ^{6}Li observation. This model is done in the framework of a hierarchical structure formation scenario, as described in Daigne et al. (2006). Rollinde et al. (2008, hereafter RVOII) have also examined specifically the consequences of the CCR production of ^{6}Li on the abundances of the related Be and B isotopes, as well as on the abundance of D in the IGM and on the extra-galactic γ-ray background (EGRB) produced by the same processes.

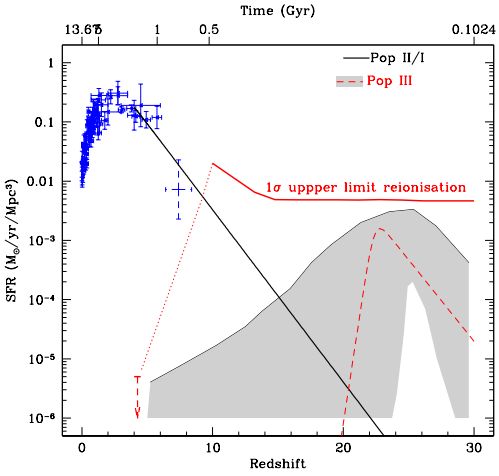

Fig. 1. Cosmic SFR as a function of redshift. The solid line is a fit of the PopII/I SFR on all the data (blue crosses, taken from Hopkins & Beacom, 2006; Bouwens et al., 2007). The grey area and dashed line correspond to the PopIII SFR adjusted using the WMAP5 upper limit on the Thomson optical depth (Figure 2) and constraints from star abundances (Figure 3).

An overview of the cosmological scenario is given in Section 2, including the hierarchical model of structure formation and the different observational constraints on PopIII stars formation rate and the associated mass ranges. We describe the CCR production of ^{6}Li in the IGM in Section 3, and the consequences on the formation of D, Be, B and γ-rays are given.

2. Hierarchical structure formation and PopIII stars

Daigne et al. (2006) have developed a detailed model of cosmological chemical evolution, using a simplified description of structures, based on the standard Press-Schechter (PS) formalism (Press & Schechter, 1974; Sheth & Tormen, 1999; Jenkins et al., 2001). On top of this, we consider two distinct modes of star formation: a normal mode of PopII/I stars and a massive mode of PopIII stars.

This model was developed with a primordial power spectrum, $P(k) \propto k^n$, with a power law index $n = 1$ and the cosmological parameters of Spergel et al. (2003), i.e. Ω_m =

0.27, $\Omega_\Lambda = 0.73$, $\Omega_b = 0.044$, $h = 0.71$ and $\sigma_8 = 0.9$. Yet, we have updated the observational constraints on the reionisation by Komatsu et al. (2011).

The Star Formation Rate (SFR) data compiled in Hopkins & Beacom (2006) (from $z = 0$ to 5), and the recent measurement at $z \sim 7$ by Bouwens et al. (2007) are well adjusted with one single fit assuming only PopII/I stars (see Figure 1), with a Salpeter Initial Mass Function (IMF). Chemical evolution of massive stars is followed thanks to the yields of Woosley & Weaver (1995). The SFR of PopIII stars, as well as their mass ranges (or IMF) are not directly observable and we discuss below different constraints that yield to the shaded area. Indeed, the role of massive PopIII stars is presently poorly understood. Thus, the mass range of these stars is an open question. Yet, as PopIII stars are the primary source for the early metal enrichment of the interstellar medium (ISM) as well as for the intergalactic medium (IGM), it is possible to set constraints on this mass range thanks to nucleosynthesis calculation (see details in Rollinde et al., 2009, hereafter RVOIII).

Having set different SFR and IMF in our model (both for PopII/I and PopIII stars), we compute the evolution of the abundances of different elements in ISM and in IGM and we calculate the electron scattering optical depth, following the different prescriptions in Greif & Bromm (2006) (for details, see Daigne et al., 2006, and RVOIII).

2.1. Reionization constraints

In Figure 2, we show the integrated optical depth from $z = 0$ to z. The prediction from the normal mode only (black thick solid curve) is contained in the 1σ WMAP limit (grey band). A mode with massive PopIII stars at high redshift only makes it easier to reproduce the optical depth (dashed curve). We note that only an upper limit on the integral of the SFR is constrained by this observation, which explains the upper limit in Figure 1.

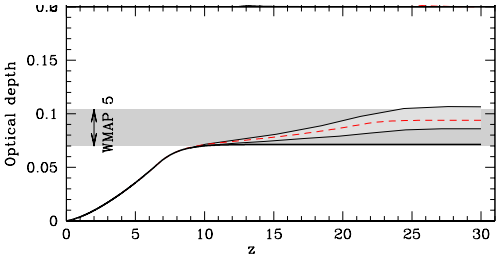

Fig. 2. Integrated Thomson optical depth with and without PopIII stars (dashed and thick solid black respectively). The thin lines frame the optical depth evolution for different models of PopIII stars that reproduce the chemical abundance constraints (Figure 3). The range of allowed values for the optical depth as measured by WMAP5 (Dunkley et al., 2009) is also shown.

2.2. Abundances of halo stars

We focus on the giants of the ESO-LP Cayrel et al. (2004), which contains 35 very metal-poor stars (VMPS). Since the iron abundance is not the best tracer of star formation, Bromm & Loeb (2003) have defined a *transition discriminant* to take into account the predominant role of carbon and oxygen; $D_{\rm trans} \equiv \log_{10}(10^{[C/H]} + 0.3 \times 10^{[O/H]})$. Figure 3 shows the location of the ESO-LP VMPS (circles) in a scatter plot of $D_{\rm trans}$ versus [Fe/H]. RVOIII also included in their analysis three metal-poor stars (lower triangles) that have been observed: HE0107-5240 (Christlieb et al., 2002), HE1327-2326 (Frebel et al., 2005; Aoki et al., 2006) and HE 1300+015 (upper triangle Frebel et al., 2007). The distinction between the three peculiar Carbon-Rich Extremly Metal Poor stars (CEMPS) and the bulk of the ESO-LP stars is made clear with this figure. Remind that those abundances are derived from the analysis of absorption lines and are still subject to large uncertainties.

As we follow the C, O and Fe abundance evolution, we calculate $D_{\rm trans}$ at each redshift. The evolution of $D_{\rm trans}$ versus [Fe/H] from $z = 30$ to $z = 0$ is shown (different curves). The ESO-LP observations are well reproduced for a standard IMF as used for the normal mode (thick solid line). The evolution of $D_{\rm trans}$ when including the massive mode is more complex

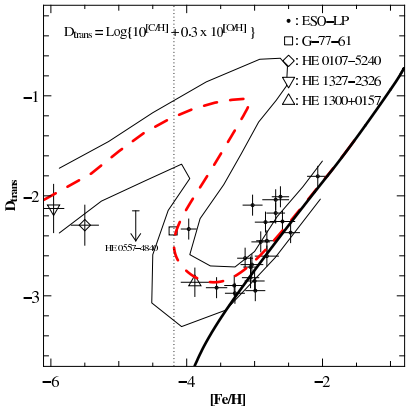

Fig. 3. The transition discriminant, $D_{\rm trans}$, for metal-poor stars as a function of [Fe/H]. The ESO-LP stellar data are shown as circles while peculiar CEMP stars are indicated with different symbols. The thick black solid line corresponds to a model with PopII/I stars alone. The addition of PopIII stars (30-100 $M_\odot$, our best model) leads to the dashed line. The dotted line indicates the minimum metallicity that should be observed for standard, i.e. not carbon rich, metal-poor stars.

(dashed line and envelope). At high redshift, those stars eject Carbon and Oxygen, but no Iron. As the SFR of PopIII stars is reduced (see Figure 1 and details in RVOIII) the accretion of pristine IGM material continues, leading to the dilution of ISM abundances. Then, $D_{\rm trans}$ and [Fe/H] decrease simultaneously until the onset of PopII/I stars. This pattern allows one to reproduce simultaneously observations of CEMPS at high redshift and of ESO-LP stars at low redshift. As a result, these specific stars must indeed be associated with stars formation occurring within regions having a specific nucleosynthetic history at early times (due to ejecta of PopIII stars) as suggested in Frebel (2008).

Finally, the constraints on the SFR and IMF of PopIII stars from the CEMPS abundances are already sufficient to prove the presence of massive stars at high redshift. To reproduce the abundances of halo stars, the ejecta of metals from PopIII stars must be in lack of iron. This constrains the mass range to be of the order of tenths of $M_\odot$. We can now proceed and use this specific scenario to investigate the production of LiBeB by Cosmological Cosmic Rays.

3. Cosmological cosmic rays

The production of CRs is directly related to the detailed model of cosmic chemical evolution in which the SN history is completely determined by the SFR and IMF. We are interested here in the production of CRs in the IGM. Then, one has to discuss the CR confinement in the structure first. We define ϵ_{esc} as the fraction of energy in CRs that escapes in the IGM. The exact evolution of CR confinement is difficult to estimate, Ensslin (2003) discusses the relation of the diffusion coefficient with a magnetic field. Jubelgas et al. (2008) propose a simple model where this coefficient varies as the inverse of the square root of the density. The efficiency of the diffusion will then decrease with the density (as could be intuitively inferred). Then, at large redshift, the structures are smaller, possibly less dense and the primordial magnetic field could be expected to confine less than it does today, which corresponds to a large value for ϵ_{esc}. In this context, we will assume that ϵ_{esc} = 1, bearing in mind that this approximation should not be valid at low redshift (z < 3). Our results for the primitive production of LiBeB will depend on the product of the CR escape efficiency, ϵ_{esc}, and the efficiency for converting SN energy into CRs, ϵ.

3.1. Production of ^{6}Li

We can derive the abundance of Lithium produced in the IGM by the interaction between α CRs and He at rest in the IGM. We assume that the IGM abundances act as a prompt initial enrichment (PIE) for the halo stars when the galaxy forms (at $z \sim 3$). The observed ^{6}Li plateau at low metallicity is assumed to originate solely from production in the IGM by those cosmological CRs, which sets the single free parameter ϵ as described now.

In Figure 4, we show the evolution of the Li abundances for ϵ_{esc} = 1 with different models of PopIII stars. In the model with PopIII stars of mass 30-100 $M_\odot$ (model 1) the CR efficiency, ϵ has been fixed at ϵ = 0.15 so that

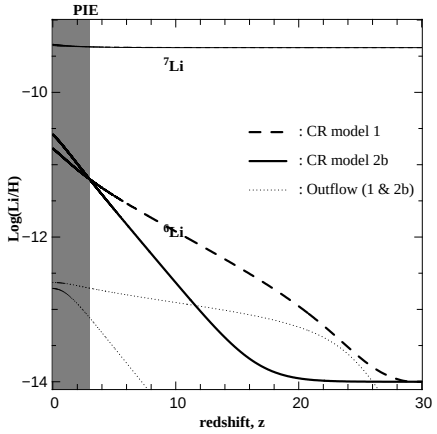

Fig. 4. Nucleosynthesis of both isotopes of lithium through the interactions of CCR α particles impinging on He in the IGM including the enrichment via the outflows of ISM into the IGM (thick lines: total; thin lines: outflows only). Model 2b and Model 1 correspond to very massive PopIII stars (> 500$M_\odot$) without metal ejecta and 30-100 $M_\odot$ PopIII stars respectively. We impose a PIE at $z = 3$ which equals the observed plateau ^{6}Li/H=$10^{-11.2}$.

the total amount of Lithium produced at $z = 3$ is ^{6}Li/H =$10^{-11.2}$, a value perfectly consistent with the observations of ^{6}Li in halo stars. Note that, as claimed in RVOI, ^{7}Li is not overproduced by this process.

In a model with very massive PopIII stars (500 $M_\odot$, model 2b), those can still help for reionization, but do not eject any metal (the abundances of C-EMPS will not be reproduced then). Since PopII/I stars must produce ^{6}Li alone, it yields to a larger value of $\epsilon = 0.5$.

3.2. Beryllium, boron, deuterium and EGRB

Beryllium and boron are produced via spallative interaction between *i)* protons or α's in CRs and CNO elements in the IGM and *ii)* by the reverse reactions, which correspond to CNO CRs spalling on H and He of the IGM. This last process is in fact dominant in this cosmological context. This can be understood as the metallicity in the ISM (where CRs originate) is always larger than that in the IGM. For each model of SFR and IMF of PopIII stars, ϵ is fixed to reproduce the PIE of ^{6}Li. The evolution of ^{9}Be model is thus constrained in our model. It rises earlier in model 1 than in model 2b, but PopII/I stars are sufficient to produce a non-negligible amount of ^{9}Be and B. At $z = 3$, we find ^{9}Be/H= $10^{-12.9}$ in model 1 and ^{9}Be/H= $10^{-13.3}$ in model 2b. Most recent observations (Rich & Boesgaard, 2009) may indicate a flattening of the evolution of ^{9}Be/H versus [Fe/H]; yet, the reality of this feature depends on the input stellar parameters used for the analysis (Primas, 2010; Boesgaard et al., 2010). The observed abundance at the lowest metallicity, [Fe/H]~ -3.3, would then indicate a PIE of ^{9}Be/H$\sim 10^{-13.2}$ consistent with our prediction. For boron, the analysis and observation at low metallicity is more difficult (see contributions in 2010 IAU Symposium, e.g. Primas, 2010). The observed abundance (Primas et al., 1999) is typically B/H$\sim 10^{-11.3}$ at [Fe/H]= −3.0, which is somewhat above the predicted CCR production of B/H = $10^{-11.9}$ in model 1 and and B/H = $10^{-12.25}$ in model 2b (RVOII).

There are two main production reactions for deuterium, namely pH and pHe, and similar reverse process αp. The additional production of deuterium by CCRs at $z = 3$ is about 3.1×10^{-10} and is therefore well below the observed abundance in DLAs D/H$\sim 2.82^{+0.20}_{-0.19} \times 10^{-5}$ (O'Meara et al., 2006; Pettini et al., 2008). The interaction of the CCRs with the IGM also produces gamma-rays. The same input fluxes and IGM densities are taken as for the D and LiBeB calculations. We find that the total γ-ray flux produced by CCRs ($IE^2 < 10^{-6.8}$ GeV^2(cm^2 s GeV sr)$^{-1}$; Figure 7 of RVOII) is negligible compared to the observed EGRB (Strong et al., 2007).

In conclusion, our model of cosmological cosmic rays allows for a pre-galactic production of LiBeB. This may explain observations of different early plateaus in the evolution of LiBeB abundances with metallicity, without producting Deuterium, gamma-rays and ^{7}Li in excess. We are now waiting for additional data one one side, and more theoretical constraints on CR production at high redshift on the other side. The scenario of cosmological evolution

that we have developed will then be useful as a link between both sides.

References

Aoki, W., et al. 2006, in American Institute of Physics Conference Series, Vol. 847, Origin of Matter and Evolution of Galaxies, ed. S. Kubono, W. Aoki, T. Kajino, T. Motobayashi, & K. Nomoto, 53–58

Asplund, M., et al. 2006, ApJ, 644, 229

Boesgaard, A. M., Rich, J. A., Levesque, E. M., & Bowler, B. P. 2010, in , 231–236

Bouwens, R. J., Illingworth, G. D., Franx, M., & Ford, H. 2007, ApJ, 670, 928

Bromm, V. & Loeb, A. 2003, Nature, 425, 812

Cayrel, R., 2007, A&A, 473, L37

Cayrel, R. et al. 2004, A&A, 416, 1117

Christlieb, N., et al. 2002, Nature, 419, 904

Coc, A., et al. 2011, astro-ph/1107.1117

Coc, A. & Vangioni, E. 2010, Journal of Physics Conference Series, 202, 012001

Cyburt, R. H., Fields, B. D., & Olive, K. A. 2008, J. Cosmology Astropart. Phys., 11, 12

Daigne, F., Olive, et al. 2006, ApJ, 647, 773

Dunkley, J., et al. 2009, ApJS, 180, 306

Ensslin, T. 2003, A&A, 399, 409

Frebel, A. 2008, ArXiv e-prints, 802

Frebel, A., et al. 2005, in , 1272

Frebel et al., A. 2007, ApJ, 658, 534

Greif, T. H. & Bromm, V. 2006, MNRAS, 373, 128

Hammache, F., et al. 2010, Phys. Rev. C, 82, 065803

Hopkins, A. M. & Beacom, J. F. 2006, ApJ, 651, 142

Inoue, S., et al. 2005, in IAU Symposium, Vol. 228, From Lithium to Uranium: Elemental Tracers of Early Cosmic Evolution, ed. V. Hill, P. François, & F. Primas, 59–64

Jenkins, A., et al. 2001, MNRAS, 321, 372

Jubelgas, M., et al. 2008, A&A, 481, 33

Komatsu, E., et al. 2011, ApJS, 192, 18

O'Meara, J. M., et al. 2006, ApJ, 649, L61

Pettini, M., et al. 2008, MNRAS, 391, 1499

Press, W. H. & Schechter, P. 1974, ApJ, 187, 425

Primas, F. 2010, in , 221–230

Primas, F., et al. 1999, A&A, 343, 545

Rich, J. A. & Boesgaard, A. M. 2009, ApJ, 701, 1519

Rollinde, E., et al. 2008, ApJ, 673, 676

Rollinde, E., et al. 2009, MNRAS, 398, 1782

Rollinde, E., Vangioni, E., & Olive, K. A. 2006, ApJ, 651, 658

Sbordone, L., et al. 2010, A&A, 522, A26

Sheth, R. K. & Tormen, G. 1999, MNRAS, 308, 119

Spergel, D. N., et al. 2003, ApJS, 148, 175

Spite, M. & Spite, F. 2010, in , 201–210

Steffen, M., et al. 2010, in , 23–26

Strong, A. W., Moskalenko, I. V., & Ptuskin, V. S. 2007, Annual Review of Nuclear and Particle Science, 57, 285

Vangioni-Flam, E., Cassé, M., & Audouze, J. 2000, Phys. Rep., 333, 365

Woosley, S. E. & Weaver, T. A. 1995, ApJS, 101, 181